MOSS, S. C. (1966). *Local Atomic Arrangements Studied by X-ray Diffraction.* Edited by J. B. COHEN and J. E. HILLIARD. pp. 95–122. New York: Gordon and Breach.
MOSS, S. C. (1969). *Phys. Rev. Lett.* **22**, 1108–1111.
MOSS, S. C. & CLAPP, P. C. (1968). *Phys. Rev.* **171**, 764–777.
OGAWA, S., IWASAKI, H. & TERADA, A. (1973). *J. Phys. Soc. Japan.* **34**, 384–390.
PEARSON, W. B. (1958). *A Handbook of Lattice Spacings and Structures of Metals and Alloys.* Oxford: Pergamon Press.
RAETHER, H. (1952). *Angew. Phys.* **4**, 53–59.
ROBERTS, B. W. (1954). *Acta Met.* **2**, 597–603.
SATO, H. & TOTH, R. S. (1961). *Phys. Rev.* **124**, 1833–1847.
SATO, H. & TOTH, R. S. (1962). *Phys. Rev.* **127**, 469–484.
SATO, K., WATANABE, D. & OGAWA, S. (1962). *J. Phys. Soc. Japan*, **17**, 1647–1651.
SCATTERGOOD, R. O., MOSS, S. C. & BEVER, M. B. (1970). *Acta Met.* **18**, 1087–1098.
SCHNEIDER, A. & ESCH, U. (1944). *Z. Elektrochem.* **50**, 290–301.
SCHUBERT, K., KIEFER, B., WILKENS, M. & HAUFLER, R. (1955). *Z. Metallk.* **46**, 692–715.
TACHIKI, M. & TERAMOTO, K. (1966). *J. Phys. Chem. Solids*, **27**, 335–348.
WALKER, C. B. (1952). *J. Appl. Phys.* **23**, 118–123.
WATANABE, D. (1959). *J. Phys. Soc. Japan*, **14**, 436–443.
WATANABE, D. & FISHER, P. M. J. (1965). *J. Phys. Soc. Japan*, **20**, 2170–2179.
WATANABE, D. & OGAWA, S. (1956). *J. Phys. Soc. Japan*, **11**, 226–239.
WILKINS, S. (1970). *Phys. Rev.* B**2**, 3935–3942.

Acta Cryst. (1973). A**29**, 526

On the Use of in-Pile Collimators in Inelastic Neutron Scattering

BY J. KALUS

Physik-Department der Technischen Universität München, 8000 *München, Arcisstrasse* 21, *Germany (BRD)*

AND B. DORNER*

Institut Max von Laue–Paul Langevin, B.P. 156, 38042-*Grenoble Cedex, France*

(*Received* 16 *January* 1973; *accepted* 28 *March* 1973)

The influence of an in-pile collimator is shown for two cases: *A*. Divergence α_0 of the incoming beam large compared to the mosaic width η of the monochromating crystal and the divergence α_1 after the crystal ($\alpha_0 > \eta, \alpha_1$). *B*. $2\eta > \alpha_0, \alpha_1$. If the same energy resolution for a three-axis spectrometer is required, an optimized comparison of the counting rates in these two cases reveals a factor of *two* in favour of case *B*. This is an important reduction in measuring time for investigations of horizontal dispersion branches, for quasielastic and incoherent scattering, where only the energy (no momentum) resolution is concerned.

1. Introduction

The impression that an in-pile collimator is useless was gained in many discussions the authors have had with scientists performing inelastic neutron-scattering experiments. Therefore we looked into this problem in more detail and found that it is indeed very useful in many cases.

For inelastic neutron-scattering experiments performed with a three-axis spectrometer one uses Bragg reflexion for the monochromation and analysis of the neutrons.

The Bragg law is

$$k = \frac{\pi}{d \cdot \sin \theta_B} \qquad (1)$$

where k is the wave number of the Bragg scattered neutrons, θ_B the Bragg angle and d the spacing of the reflecting lattice planes.

The distribution of the Bragg-reflected neutrons, characterized by the distribution of wave vectors **k**, depends on the collimations α_0 and α_1 before and after reflexion and on the mosaic width η in the crystal. This holds for the monochromator as well as for the analyser.

In the following sections we discuss the cases $\alpha_0 > \eta, \alpha_1$ and $2\eta > \alpha_0, \alpha_1$. For these two cases the shape of the **k** distribution of the reflected neutrons changes appreciably. In § 4 we show that the counting rate of a three-axis spectrometer is different for these two cases. Given a certain overall energy resolution of the apparatus we make an optimization by looking for the best set of the parameters α_0, α_1 and η for the two cases.

2. Case *A*. Neutron monochromation for $\alpha_0 > \eta, \alpha_1$

The hatched region in Fig. 1 shows the momentum distribution of the Bragg-scattered neutrons having a collimator for the incoming neutrons only, characterized by the collimation angle α_0. The distribution of the **k** vectors, taken across the incoming white neutron beam, is indicated by the dotted area. The effect of a second collimator for the scattered neutrons, characterized by the collimation angle α_1 is shown by cross hatching in the reflected beam only.

* On leave from Institut für Festkörperforschung, KFA-Jülich, Germany (BRD).

Provided the collimator angle α_1 of the latter collimator is given by

$$0 \leq \alpha_1 < \alpha_0 - 2\eta \tag{2}$$

the momentum distribution of the neutrons impinging, for example, on a sample is limited in the simple way shown in Fig. 1. The uncertainty of $\mathbf{k}$ in beam direction is given by:

$$\frac{\Delta \mathbf{k}}{\mathbf{k}} = \eta \,.\, \cot \theta_B . \tag{3}$$

3. Case *B*. Neutron monochromation for $2\eta > \alpha_0, \alpha_1$

The symbols for the different momentum distributions of the neutrons in Fig. 2 for the case $\eta \gg \alpha_0/2$ correspond to those in Fig. 1.

The orientation of the momentum distribution of the Bragg-scattered neutrons is governed by an angle θ:

$$\tan \theta = 2 \tan \theta_B . \tag{4}$$

Instead of equation (2) we find now:

$$0 \leq \alpha_1 < 2\eta - \alpha_0 \tag{5}$$

and for equation (3):

$$\frac{\Delta \mathbf{k}}{\mathbf{k}} = \frac{\alpha_0}{2} \cot \theta_B = \alpha_0 \,.\, \cot \theta . \tag{6}$$

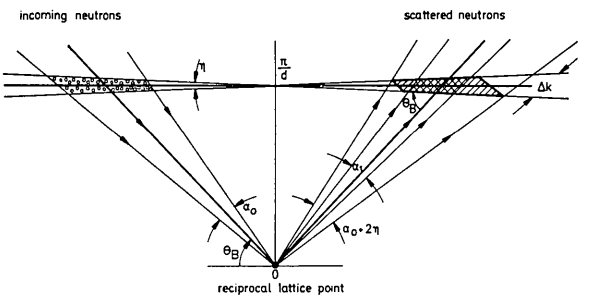

Fig. 1. Bragg reflexion at a single crystal with a mosaic angle η smaller than half the collimation α_0 of the incoming neutrons. α_1 defines the collimation of the scattered neutrons. θ_B is the Bragg angle.

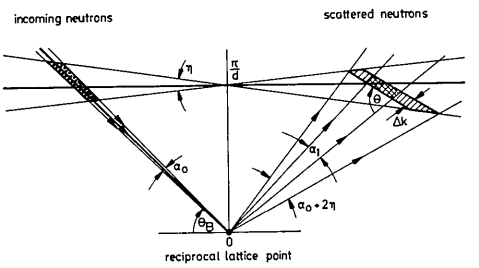

Fig. 2. Bragg reflexion at a single crystal with a mosaic angle η larger than the collimation α_0 of the incoming neutrons. α_1 defines the collimation of the scattered neutrons.

4. Counting rate for a given energy resolution of a three-axis spectrometer

In, for example, an incoherent inelastic neutron-scattering experiment one can match the energy uncertainty ΔE_0 of the neutrons striking the sample to the energy uncertainty ΔE_1 of the neutrons accepted by the analyser. The highest counting rate for a given overall energy resolution is achieved if the relation $\Delta E_1 = \Delta E_0 = \Delta E$ is fulfilled. In further discussion we assume that this matching has been done. We concentrate on the question of how the counting rate differs for the two arrangements described in §§ 2 and 3. For each of these cases we will determine the best set of α_0, α_1 and η, giving the highest counting rate for the given overall energy resolution. We discuss the optimization for the monochromator (ΔE_0) first.

The energy uncertainty of the neutrons striking a sample (see Appendix) is given by:

$$\left(\frac{\Delta E}{E}\right)_A = 2 \cot \theta_B \,.\, \sqrt{\eta_A^2 + \alpha_{1A}^2} \tag{7}$$

for case A and

$$\left(\frac{\Delta E}{E}\right)_B = 2 \cot \theta \sqrt{\alpha_{0B}^2 + \alpha_{1B}^2} = \cot \theta_B \sqrt{\alpha_{0B}^2 + \alpha_{1B}^2} \tag{8}$$

for case B. Here we assumed a Gaussian law for the mosaic distribution as well as for the transmission function of the collimators, whereas the Figures are drawn for rectangular distributions for clarity.

The counting rate I is proportional to the area F of the cross-hatched region in Figs. 1 and 2. (The vertical divergence is left out of the discussion). This area F is connected generally (Dorner, 1972) to the horizontal divergences and mosaic width by:

$$F \simeq \frac{\alpha_0 \,.\, \alpha_1 \,.\, \eta}{\sqrt{\alpha_0^2 + \alpha_1^2 + 4\eta^2}} . \tag{9}$$

An optimization of this area by considering equations (7) and (8) gives:

$$\eta_A = \alpha_{1A} \tag{10}$$

for case A and

$$\alpha_{0B} = \alpha_{1B} \tag{11}$$

for case B.

Putting

$$\left(\frac{\Delta E}{E}\right)_A = \left(\frac{\Delta E}{E}\right)_B$$

we get:

$$\eta_A = \tfrac{1}{2}\alpha_{0B} \tag{12}$$

and for the counting rates I_A for case $A(\alpha_{0A}$ very large) and I_B for case $B(\eta_B$ very large)

$$F_A = \alpha_{1A} \,.\, \eta_A , \quad F_B = \tfrac{1}{2}\alpha_{0B} \,.\, \alpha_{1B} , \quad I_B = 2I_A . \tag{13}$$

In Fig. 3 we give a picture of the momentum distributions for cases A and B for the optimized conditions.

The energy uncertainty of the neutrons is given in Fig. 3 by $\Delta E/E=2\Delta\mathbf{k}/\mathbf{k}$. The result of equation (13) holds for incoherent scattering experiments as well as for coherent one-phonon scattering, provided one has a horizontal dispersion curve.

Within the framework described by Kalus (1973) the result of equation (13) can be generalized for the case of dispersion curves which are not flat.

One finds:

$$I_B=2\left|1-\frac{1}{2+\cot\theta_B\,.\,\cot\bar{\eta}_0}\right|\,.\,I_A\,. \qquad (14)$$

The angle $\bar{\eta}_0$ is related in a simple way to grad ω. Grad ω is the steepness of the dispersion curve ($\bar{\eta}_0$ is equal to zero for grad $\omega=0$). It was further assumed that the vector grad ω lies in the scattering plane.

For the analyzer system of the three-axis spectrometer the above considerations for the monochromator system can be repeated. This means that one can gain a further factor of two in the counting rate by changing from an analyser of type A to one of type B. This holds generally even for ΔE_0 very different from ΔE_1. Of course, one always tries to match $\Delta E_0\simeq\Delta E_1$.

5. Conclusion

The use of case B has some advantages, because one can optimize in a predetermined way the shape of the momentum volume $\mathbf{k}$ by just changing the collimation, using always the same crystal with a relatively high mosaic angle. For flat dispersion curves the advantage is quite evident, while for general dispersion curves one can determine by means of equation (14), which of the two cases A and B is better suited.

Case B is very well suited for a double-monochromator system with one collimator between the two crystals (defining α_0) and the other after the second crystal (defining α_1). In this case the replacement of the 'in-pile' collimator, which defines α_0, is very easy to achieve.

We wish to thank Dr M. T. Hutchings for helpful discussions.

APPENDIX

To derive an expression for $\Delta E/E=2\Delta k/k$ after a monochromating or analysing system we write the horizontal distribution P of neutrons for a monochromator as given by Cooper & Nathans (1967):

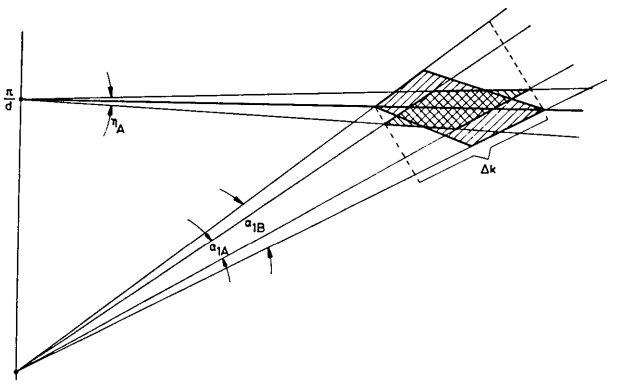

Fig. 3. Shape of the momentum elements of the scattered neutrons for the optimized cases A and B described in the text. $\Delta\mathbf{k}$ defines the energy resolution *via* $\Delta E/E=2\Delta K/K$.

$$P(\Delta\mathbf{k}_i,\gamma_1)\simeq\exp\left\{-\left[\frac{(\Delta\mathbf{k}_i/\mathbf{k}_I)\tan\theta_M+\gamma_1}{\eta_M}\right]^2+\left[\frac{2(\Delta\mathbf{k}_i/\mathbf{k}_I)\tan\theta_M+\gamma_1}{\alpha_0}\right]^2+\left(\frac{\gamma_1}{\alpha_1}\right)\right\}^2 \qquad (A1)$$

where γ_1 is an angular variable in the divergence of the outgoing beam (width α_1). After integrating equation (A1) over γ_1 we find:

$$P(\Delta k_i)\simeq\exp\left\{-\frac{\alpha_0^2+\alpha_1^2+4\eta^2}{\alpha_0^2\alpha_1^2+\alpha_0^2\eta^2+\alpha_1^2\eta^2}\times[(\Delta\mathbf{k}_i/\mathbf{k}_I)\tan\theta_M)^2\right\} \qquad (A2)$$

which gives

$$\frac{\Delta E_i}{E_I}=2\,\frac{\Delta\mathbf{k}_i}{\mathbf{k}_I}=2\cot\theta_M\left(\frac{\alpha_0^2\alpha_1^2+\alpha_0^2\eta^2+\alpha_1^2\eta^2}{\alpha_0^2+\alpha_1^2+4\eta^2}\right)^{1/2}. \qquad (A3)$$

Equation (A3) can as well be derived from the considerations of Bjerrum Møller & Nielsen (1970).

References

BJERRUM MØLLER, H. & NIELSEN, M. (1970). *Instrumentation for Neutron Inelastic Scattering Research*, pp. 49–76, Vienna: IAEA.

COOPER, M. J. & NATHANS, R. (1967). *Acta Cryst.* **23**, 357–367.

DORNER, B. (1972). *Acta Cryst.* A**28**, 319–327.

KALUS, J. (1973). *Kerntechnik*, **15**, 228–230.